Proc. Natl. Acad. Sci. USA
Vol. 93, pp. 11213–11218, October 1996
Neurobiology

Selective inhibition of Alzheimer disease-like tau aggregation by phenothiazines

(paired helical filament/prion-like/amyloidosis/prophylactic treatment)

C. M. WISCHIK*, P. C. EDWARDS*, R. Y. K. LAI*, M. ROTH†, AND C. R. HARRINGTON*

*Cambridge Brain Bank Laboratory, University Department of Psychiatry and Medical Research Council Laboratory of Molecular Biology, Medical Research Council Centre, Hills Road, Cambridge CB2 2QH, United Kingdom; and †Trinity College, Cambridge CB2 1TQ, United Kingdom

Communicated by Aaron Klug, Medical Research Council Laboratory of Molecular Biology, Cambridge, United Kingdom, July 19, 1996 (received for review March 7, 1996)

ABSTRACT **In Alzheimer disease (AD) the microtubule-associated protein tau is redistributed exponentially into paired helical filaments (PHFs) forming neurofibrillary tangles, which correlate with pyramidal cell destruction and dementia. Amorphous neuronal deposits and PHFs in AD are characterized by aggregation through the repeat domain and C-terminal truncation at Glu-391 by endogenous proteases. We show that a similar proteolytically stable complex can be generated *in vitro* following the self-aggregation of tau protein through a high-affinity binding site in the repeat domain. Once started, tau capture can be propagated by seeding the further accumulation of truncated tau in the presence of proteases. We have identified a nonneuroleptic phenothiazine previously used in man (methylene blue, MB), which reverses the proteolytic stability of protease-resistant PHFs by blocking the tau–tau binding interaction through the repeat domain. Although MB is inhibitory at a higher concentration than may be achieved clinically, the tau–tau binding assay was used to identify desmethyl derivatives of MB that have K_i values in the nanomolar range. Neuroleptic phenothiazines are inactive. Tau aggregation inhibitors do not affect the tau–tubulin interaction, which also occurs through the repeat domain. Our findings demonstrate that biologically selective pharmaceutical agents could be developed to facilitate the proteolytic degradation of tau aggregates and prevent the further propagation of tau capture in AD.**

In Alzheimer disease (AD) the axonal microtubule-associated protein tau is redistributed into paired helical filaments (PHFs) (1–4). PHFs containing full-length and truncated tau accumulate in the somatodendritic compartment of pyramidal cells as dystrophic neurites and neurofibrillary tangles (5–8). Neuronal loss and dementia are both correlated with the extent of neurofibrillary pathology (9–12). The molecular mechanisms responsible for PHF assembly are poorly understood (13). Several studies have shown that tau protein can form polymers *in vitro* (14–20). A feature common to assembly-competent fragments is the presence of the tandem repeat region. Tau fragments from PHFs encompassing this region form detergent-resistant dimers and trimers *in vitro* (1, 21, 22), and proteolytic digestion of extracts from PHF preparations leads to enhanced aggregation of tau fragments containing the repeats (23). It has been proposed that aggregation involves anti-parallel dimerization (15) under nonreducing conditions (24), whereas others have reported reducing conditions as necessary for filament assembly (25). The relevance of these findings for understanding PHF assembly *in vivo* has not been established.

In this paper, we report the results of work aiming to reproduce *in vitro* aspects of the pathological processing of tau protein in the human brain, which we have defined in earlier structural (26–28), biochemical (1, 21), immunological (2, 29, 30), molecular (22, 31), and clinico-pathological (3, 4, 32, 33) studies. The proteolytically stable core of the PHF left after exogenous proteolysis contains a 93-amino acid residue fragment from the repeat domain of tau (1). A monoclonal antibody (mAb 423), raised against PHFs, recognizes only those recombinant analogues of core fragments that terminate at Glu-391 (22). This truncation and the known N termini of the native core fragments define a 14-residue phase shift relative to the tubulin-binding repeats (21, 22). mAb 423 recognizes truncated tau in amorphous tau deposits at early stages of pathology (7, 8), in intracellular PHFs *in situ* (5, 7, 8), and in PHFs isolated in the absence of exogenous proteases (22, 28). As the core fragment is proteolytically sensitive once released from PHFs (1), we have proposed that both proteolytic stability and the conformational shift associated with truncation at Glu-391 are due to aggregation through the repeat domain (1, 21, 22). We report the development of tau binding assays in physiological conditions *in vitro* to examine this hypothesis. The rationale for examining the feasibility of direct pharmaceutical inhibition of tau aggregation was based on our earlier work, now reported for the first time, showing that certain compounds reverse the proteolytic stability of the tau fragment within protease-resistant PHFs.

MATERIALS AND METHODS

Proteins and mAbs. Full-length recombinant tau protein (T: 441-residue isoform, clone htau40), produced and isolated as described (34), was phosphorylated (TP) *in vitro* by the method of Biernat *et al.* (35). Truncated tau fragments dGA (residues 297–390) and dGAE (residues 297–391) (recombinant repeat domain tau protein fragments terminating at Ala-390 and Glu-391, respectively) have been described (ref. 22; numbering with respect to T). Depolymerized bovine tubulin was kindly donated by J. Kilmartin (Medical Research Council Laboratory of Molecular Biology, Cambridge). mAb 6.423 (mAb 423) has been described (1, 22). mAbs 27.499 and 27.342 (mAbs 499 and 342) were raised against human recombinant tau protein; hybridomas were screened for recognition of full-length tau, but not the fragments from the PHF core (36). mAb 499 recognizes a human-specific segment between Gly-14 and Gln-26, and mAb 342 recognizes a segment between Ser-208 to Pro-251 (ref. 36; see Fig. 3*C*). Protein concentrations were determined by the method of Harrington (37).

Tau Binding Assay. The tau binding assay was carried out in 96-well PVC microtiter plates, with all incubations carried out for 1 hr at 37°C. The solid-phase species was incubated at varying concentrations ranging 0–50 μg/ml in sodium carbonate buffer (50 mM, pH 9.6), washed three times with Tween 20

The publication costs of this article were defrayed in part by page charge payment. This article must therefore be hereby marked "*advertisement*" in accordance with 18 U.S.C. §1734 solely to indicate this fact.

Abbreviations: AD, Alzheimer disease; PHF, paired helical filament; dGA and dGAE, recombinant repeat domain tau protein fragments terminating at Ala-390 and Glu-391, respectively; MB, methylene blue.

(0.05%), blocked with a 2% solution of milk extract ("Marvel") in PBS (137 mM sodium chloride/10 mM phosphate/2.68 mM potassium chloride, pH 7.4), and washed as above. The aqueous-phase species was incubated in PBS containing gelatine (1%), Tween 20 (0.05%), in the presence or absence of potential chemical inhibitors (Aldrich). Pronase (Calbiochem–Novabiochem) digestion was carried out in water for 5 min. The wells were washed as above and incubated with one of the mAbs 499, 342, or 423 (hybridoma supernatant diluted with an equal volume of 2% Marvel in PBS). Bound antibody was detected as described (38). Binding and inhibitory constants with corresponding standard errors were estimated by fitting the standard expressions: $B = (B_{max} \times [T])/(K_d + [T])$ and $B = (B_{max} \times [T])/\{[T] + \{K_d \times (1 + [I]/K_i)\}\}$, to the binding data using the SYSTAT computer program (Systat, Evanston, IL). All resulting correlation coefficients were in the range $0.975 < r < 0.997$.

PHFs. Pronase-resistant PHFs were isolated from AD brain tissue and visualized by electron microscopy, as described (1, 21, 26, 28). PHFs were treated on the grid or in suspension with methylene blue (MB), Alcec Blue, or Alcian Blue (Aldrich) at concentrations of 0.01–1%. PHF fragments in the "ABCsup" preparation (21, 37, 38), which do not sediment at 10,000 × *g* for 10 min in ammonium bicarbonate (100 mM, pH 8.5), were incubated with Alcec Blue or MB (0.02%) for 10 min at room temperature and centrifuged at 10,000 × *g* for 10 min. The supernatant was removed, the pellet suspended by sonication in 2% formic acid, treated overnight at 37°C with pepsin (1 mg/ml), and centrifuged at 10,000 × *g* for 10 min. Amino acid content of portions from supernatants after dialysis against water and pellets resuspended in ammonium hydroxide was measured as previously (37). Protein fractions were separated using 10–20% gradient SDS/PAGE gels. These were either stained with Coomassie blue or immunoblotted as described using mAbs 423 or 7.51 (1, 21).

RESULTS

Solid-Phase Binding Assay. To examine the binding properties of the repeat domain of tau protein, we optimized the conditions for a solid-phase binding assay using recombinant fragments identical to those found in the PHF core (1, 21, 22). In this assay, mAb 423 immunoreactivity was detected when dGAE in the aqueous phase had bound to solid-phase dGA (Fig. 1*A*). Likewise, binding of full-length recombinant tau to the truncated fragment was detected using mAbs 342 or 499 (Fig. 1*B*). Tau–tau binding was dependent on salt concentration and pH value, being optimal in physiological PBS (Fig. 1 *B* and *C*).

Binding of Full-Length Tau to the Truncated Fragment and to Tubulin. Binding of full-length tau to dGA was dependent on the concentrations of tau species in both the solid- and aqueous-phases (Fig. 2*A*). All of the binding data could be expressed as a set of standard Langmuir curves with two empirically derived constants, B_{max} and K_d. The K_d values for the solid- or aqueous-phase species, when the other was at a saturating concentration, were 26.6 ± 7.3 nM and 22.8 ± 2.8 nM, respectively. When neonatal rat tau was used in the solid phase, the K_d for binding of full-length recombinant human tau was 18.8 ± 3.4 nM. As the K_d values for binding to full-length or truncated species were experimentally indistinguishable, the truncated tau fragment contains all that is necessary for high-affinity binding.

It has been proposed that hyperphosphorylation represents a critical modification responsible for PHF assembly (39, 40). We compared the binding of phosphorylated tau to depolymerized bovine tubulin and to the truncated tau fragment in the solid phase in similar assay conditions. Recombinant full-length tau, which had been phosphorylated *in vitro*, bound to depolymerized tubulin with a K_d value of 9.6 ± 3.2 μM,

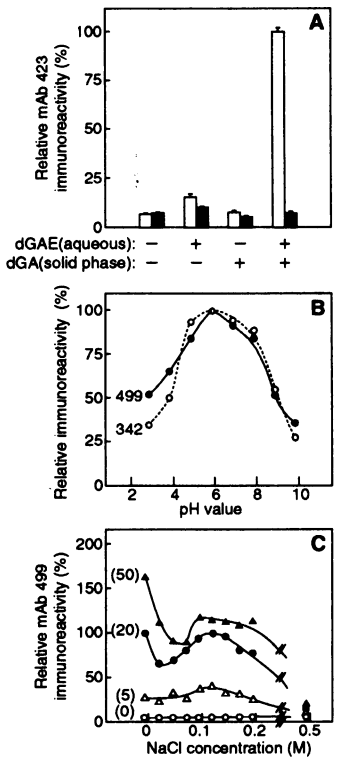

FIG. 1. Optimal conditions for the tau binding assay. (*A*) The recombinant core tau fragment terminating at Ala-390 (dGA, 10 μg/ml) was coated on the solid phase, followed by the fragment terminating at Glu-391 (dGAE, 20 μg/ml), diluted either in coating buffer (solid bars) or binding buffer (open bars) in the aqueous phase. The binding of dGAE, detected with mAb 423 (22), was dependent on the presence of dGA bound to the solid phase, whereas it did not occur when dGAE was added in the buffer used for coating dGA. (*B*) The binding of full-length recombinant tau (50 μg/ml) to dGA (20 μg/ml) was determined at different pH values, using mAbs 499 (●) and 342 (○) to detect bound tau. No immunoreactivity was detected with either antibody in the absence of full-length tau. Relative binding is shown as a percentage of bound immunoreactivity at pH 6.0 for each antibody; optimal binding occurred over the range of pH 5.0–8.0. The following buffers containing 100 mM NaCl were used: 50 mM citrate/phosphate (pH 3–6), 50 mM phosphate (pH 7–8), or 50 mM carbonate (pH 9–10). (*C*) The binding of full-length recombinant tau (0, 5, 20, or 50 μg/ml) to dGA (20 μg/ml) was determined in 10 mM phosphate buffer (pH 7.4) containing NaCl as indicated, and bound tau was detected with mAb 499. Binding occurred over the physiological range of NaCl (100–150 mM), was accentuated in the absence of NaCl, and blocked at high NaCl concentration. Data points represent means from quadruplicate measurements, with corresponding SE bars shown in *A*.

whereas for unmodified tau the K_d value for tau–tubulin binding was 403 ± 86 nM. These values correspond to those reported for the binding of tau to taxol-stabilized microtubules (35), and confirm the inhibitory effect of hyperphosphorylation on the tau–tubulin binding interaction. The K_d value for binding of phosphorylated tau to the truncated tau fragment was 252.4 ± 69.8 nM, indicating 10-fold inhibition of binding relative to the nonphosphorylated form (Fig. 2*B*). Therefore, hyperphosphorylation of tau inhibits its binding both to the truncated fragment and to tubulin in the solid phase.

Proteolytic Digestion of the Bound Tau Complex. We examined the proteolytic stability of the aggregate produced by tau–tau binding *in vitro*. Full-length recombinant tau, which had bound to dGA, acquired mAb 423 immunoreactivity in a protease concentration-dependent manner (Fig. 3*A*), and this was accompanied by the disappearance of mAb 499 and mAb 342 immunoreactivity. When full-length tau was allowed to self-aggregate during binding to the solid phase, similar

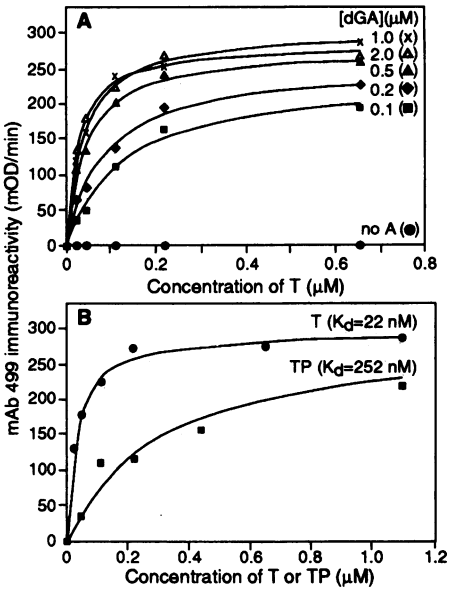

FIG. 2. Langmuir curves for binding of full-length tau protein to truncated tau. (*A*) Binding depends on the concentrations of tau species in both the solid and aqueous phases and is saturable for both. No immunoreactivity is detected in the absence of dGA or full-length tau (T). The K_d value for full-length tau, when dGA is saturating, was 22.8 ± 2.8 nM and that for dGA, when T is saturating, was 26.6 ± 7.3 nM. (*B*) Representative Langmuir curves for binding to dGA (1 μM) of purified recombinant human tau protein, which had (TP) or had not (T) been phosphorylated *in vitro*. The K_d values indicated in parentheses for T and TP at saturating concentrations of dGA were obtained from data sets for binding of each over the complete range of concentrations shown in *A*. All data points represent mean values from quadruplicate measurements.

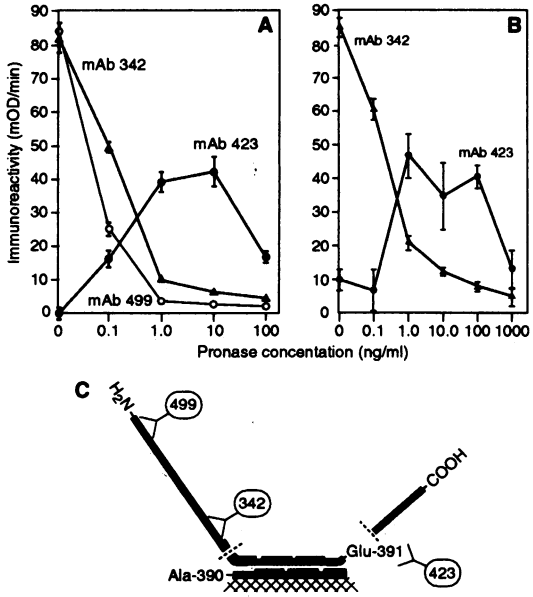

FIG. 3. Proteolytic digestion of aggregated full-length tau protein. (*A*) Full-length tau (20 μg/ml) was bound to dGA (20 μg/ml) in PBS, washed, and incubated for 5 min with Pronase in water. Immunoreactivity was measured with mAbs 342 (▲), 499 (○), and 423 (●). (*B*) Full-length tau (10 μg/ml), which had self-aggregated on the solid phase in the absence of dGA, was digested similarly and immunoreactivity measured with mAbs 342 (▲) and 423 (●). In both cases, protease concentration-dependent loss of mAb 499/342 immunoreactivity occurred concurrently with acquisition of mAb 423 immunoreactivity. Data points represent means from quadruplicate measurements, with SE bars shown. (*C*) The results from *A* are depicted schematically. The truncated fragment (dGA), initially coated on the hatched solid phase, binds full-length tau with high affinity through the repeat region, shown here to be anti-parallel (15). Proteolytic digestion of the complex (dotted lines) removes the N-terminal portion of the full-length tau molecule, with concomitant loss of the mAb 499 and 342 epitopes, and truncates it at the C terminus at Glu-391, recognized by mAb 423.

changes in immunoreactivity could be demonstrated (Fig. 3*B*). Therefore, self-aggregation confers proteolytic stability on a short segment that excludes the N-terminal half of the tau molecule and reproduces the characteristic Glu-391 truncation at the C terminus (Fig. 3*C*).

Propagation of Tau Aggregation in the Presence of Protease. The proteolytically stable fragment generated after binding and digestion *in vitro* (Fig. 4*A*) retains the capacity to capture an increased amount of full-length tau presented at the same concentration during a subsequent binding cycle (Fig. 4*B*, open bars). Repeating the process over several binding/digestion cycles (Fig. 4*C*) resulted in progressively increasing accumulation of tau protein that was C-terminally truncated at Glu-391 (Fig. 4*A*), and a corresponding increase in the binding capacity for full-length tau (Fig. 4*B*, open bars), despite complete removal of N-terminal tau immunoreactivity during the intervening digestion steps (Fig. 4*B*, solid bars). These results indicate that once the process has started, continued generation of the truncated tau fragment in the solid phase has the intrinsic capacity for propagation of tau capture in the presence of proteases.

Reversal of Proteolytic Stability of PHF Core Associated with Inhibition of Tau Aggregation. Having demonstrated the characteristics of tau binding and proteolytic stability *in vitro*, we sought to determine the feasibility of direct pharmaceutical intervention in the pathological tau–tau binding interaction. In the course of earlier work on PHF ligands (1, 41), we identified compounds able to disrupt the electron microscopic morphology of PHFs. In the presence of increasing concentrations of MB, Alcec Blue, or Alcian Blue, PHFs are seen to coarsen, swell, untwist, fragment, and disappear (Fig. 5). These changes are associated with increased susceptibility to protease digestion: 70–80% of the protein originally present in the protease-resistant PHF preparation was lost following pepsin digestion of PHFs treated with MB (Table 1). In particular, the 12-kDa fragment within the PHF core becomes sensitive to pepsin digestion (Fig. 6). By contrast, acid treatment typically releases only 10–20% of the tau protein from PHFs in a proteolytically sensitive form (1, 37).

As MB is a medicinally relevant phenothiazine (42, 43), its action was examined further *in vitro* to determine whether the effect on PHFs could be attributed to inhibition of tau–tau binding through the repeat domain. In the presence of increasing concentrations of MB, the binding of dGAE to dGA was inhibited to the point of complete blockade (Fig. 7*A*). Inhibition could be demonstrated above 30:1 molar ratio with respect to tau, with 50% inhibition seen at 150:1 molar ratio. Pepsin digestion of PHFs was demonstrated at concentrations of MB in excess of those required to achieve complete inhibition of tau–tau binding. Therefore, MB reverses the proteolytic stability of the core tau fragment within PHFs by preventing the tau–tau binding interactions needed to maintain the structure of the PHF core.

Potency, Specificity, and Selectivity of Tau Aggregation Inhibitors. Desmethyl derivatives of MB were found to be 30-fold more potent than the parent compound (Table 2). These compounds inhibited tau–tau binding by 20% at an equimolar ratio with respect to tau, and by 50% at a molar ratio of 5:1 (Fig. 7*A*). The potent inhibitors were those with the basic phenothiazine structure of 3,7-diaminophenothiazine-5-ium chloride (thionine) and derivatives partially methylated at the 3 and 7 positions (tolonium chloride, Azure A and Azure B).

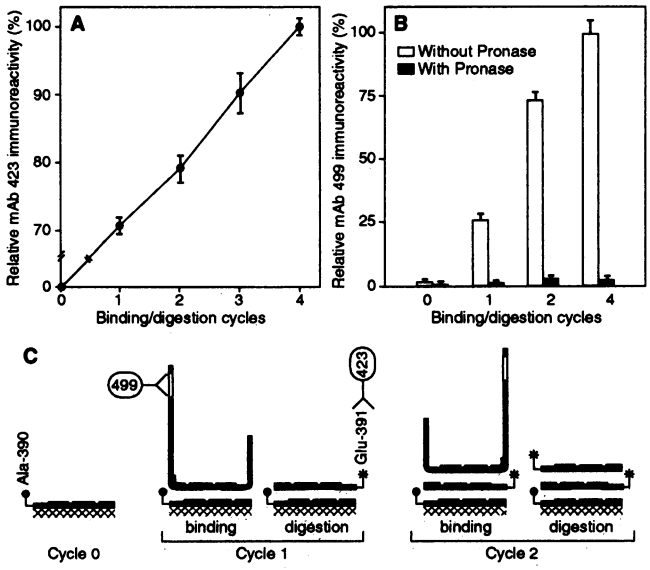

FIG. 4. Accumulation of truncated tau by repetitive tau capture. Full-length recombinant human tau (20 μg/ml) was bound to truncated tau (dGA, 20 μg/ml) on the solid phase. The aggregate was then digested with Pronase (1 ng/ml) for 5 min, washed, and the preparation was incubated with further full-length tau (20 μg/ml) and again digested. This binding/digestion cycle was repeated four times. (*A*) Pronase digestion of the complex was associated with incremental accumulation of tau protein truncated at Glu-391 following each digestion cycle. (*B*) Binding of full-length tau was detected by the appearance of mAb 499 immunoreactivity, which was entirely abolished following Pronase digestion. In the subsequent incubation cycles, binding capacity was increased for full-length tau added at a constant concentration. (*C*) These results are depicted schematically. At Cycle 0, dGA (●; not recognized by mAb 423) is bound to the solid phase. After the binding stage of Cycle 1, mAb 499 detects bound full-length tau. Following the digestion stage of Cycle 1, the N-terminal half of the tau molecule is removed (loss of mAb 499 immunoreactivity) and there is C-terminal truncation at Glu-391 (*; acquisition of mAb 423 immunoreactivity). The proteolytically stable fragment produced by digestion in Cycle 1 has the capacity to capture full-length tau during the binding stage of Cycle 2. More full-length tau is bound in Cycle 2 because there is now more truncated tau in the solid phase, and binding now saturates at a higher B_{max} (see Fig. 2*A*).

The approximation to the binding data using the calculated K_i is shown for thionine in Fig. 7*B* (●).

Not all structurally related compounds were inhibitory. Partially methylated diamino-xanthenylidines and -phenazines and had no effect on tau–tau binding (data not shown). The side groups added to the phenothiazine nucleus to achieve neuroleptic activity (e.g., chlorpromazine) abolished inhibitory activity (Fig. 7*A*, △). Likewise, the aminoacridine tacrine, was inactive (Fig. 7*A*, ■). Conversely, carbamazepine potentiated tau aggregation *in vitro* (Fig. 7*A*, □).

Table 1. Protein content in protease-resistant PHF preparation following digestion in the presence of MB

		Amino acid content, μmol
No MB	Supernatant	18.6
	Pellet	0.0
MB	Supernatant	3.1
	Pellet	10.2
MB + Pepsin	Supernatant	1.3
	Pellet	2.7

Two of the diaminophenothiazine inhibitors (thionine and Azure A) were tested for biological selectivity in the tau–tubulin binding system. No inhibition was seen when these compounds were introduced at 1000-fold excess with respect to full-length tau (Table 2; Fig. 7*B*, ○). Therefore, the tau–tau binding interactions of the PHF can be distinguished pharmaceutically from the physiological tau–tubulin binding interaction, which also occurs through the repeat domain. This is consistent with the conformational shift in the tubulin-binding repeats that is associated with truncation at Glu-391 (21, 22).

DISCUSSION

Mutations and allelic variation in several distinct gene products (44, 45), trisomy of chromosome 21 (46), and exogenous aluminium (32), are able to initiate a stereotyped cascade leading to the exponential redistribution of the tau protein pool into PHFs (4). In the medial temporal lobe, where tau pathology is particularly severe, the accelerated atrophy associated with this process can be observed by computerized tomography (47). Neuronal loss (9) and dementia (10) are both correlated with the extent of neurofibrillary pathology. Although the metabolic pathways that link the ultimate causes of AD with tau protein pathology are unknown, the incorporation of tau into PHFs necessarily requires a pathological tau–tau binding interaction through the repeat domain, and only this region of the molecule is required to maintain the proteolytically stable core of the PHF (1, 2, 21, 28–30). Features of tau capture seen in the pathological species, which accumulate as amorphous deposits and polymers within pyramidal cells in AD include aggregation through the repeat region and truncation at Glu-391 by endogenous proteases (7, 8, 22, 28).

We report an experimental system that permits the measurement of the properties of tau–tau binding through the

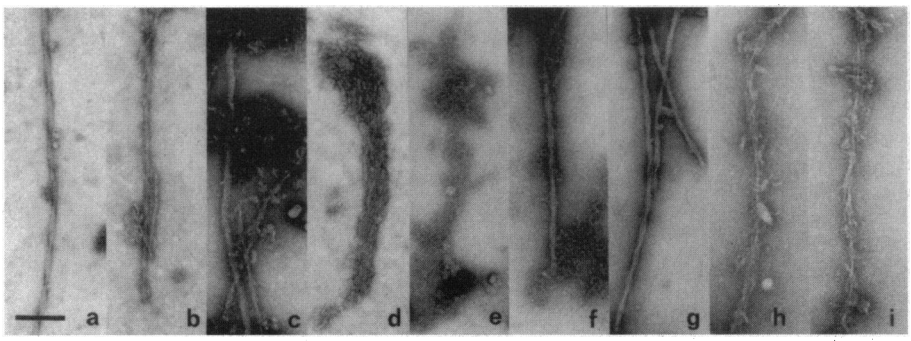

FIG. 5. Disruption of structural integrity of Pronase-resistant PHFs isolated from AD brain. PHFs are visualized by negative stain after treatment with MB (*a*, 0.01%; *b*, 0.1%; *c–e*, 1%), Alcec Blue (*f* and *g*, 0.01%), or Alcian Blue (*h* and *i*, 0.01%) by washing of partially dried PHFs on the grid (*b–d*, *f–i*) or 6-hr incubation of 100 μl aliquots (*a* and *e*). In the presence of increasing concentrations of MB, PHFs are seen to coarsen (*b* and *c*), swell (*c*), fragment (*d*), and eventually disappear after longer incubation (*e*), compared with long incubation at a lower concentration (*a*). Brief incubations on the grid with Alcec Blue and Alcian Blue produced similar results. Filament images are printed at uniform magnification. (Scale bar, 100 nm).

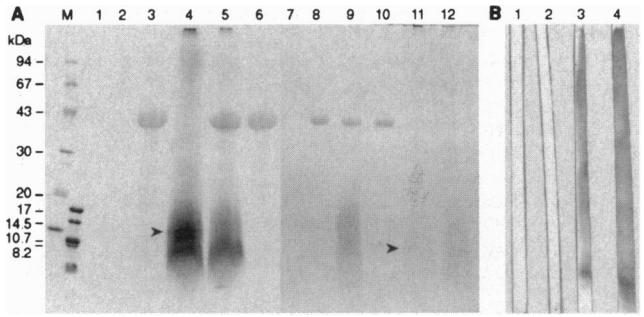

FIG. 6. Proteolytic susceptibility of the 12-kDa PHF-core tau fragment after treatment with compounds that disrupt PHF structure. (*A*) Commassie stained gels. Most of the 12-kDa tau fragment sediments at 10,000 × *g*/10′ after treatment with Alcec Blue (lane 4), and is not found in the supernatant either without (lane 2) or following (lane 3) digestion with pepsin. Pepsin digestion of the Alcec Blue pellet suspended in 2% formic acid resulted in complete removal of the 12-kDa tau fragment (lane 5), absent also from the supernatant (lane 9) or the pellet (lane 12) after digestion. Similar results were obtained with MB. The 12-kDa band is not seen in the MB supernatant (lane 7), or in the supernatant after centrifugation of the pepsin-digested MB pellet (lane 8). The pellet after pepsin digestion (lane 11) contains feint bands at 4–8 kDa, similar to those previously reported after pepsin digestion of PHFs oxidized with performic acid (21). Pepsin is shown alone (lane 6) or with MB (lane 10). (*B*) Immunoblots. None of the material in the pellet (lane 1) or supernatant (lane 2) after pepsin digestion of the MB pellet was mAb 423 immunoreactive. In the absence of compounds or pepsin, the mAb 7.51 immunoreactive 12-kDa band was found in the pellet (lane 3) and supernatant (lane 4). The relative mass of markers (lanes M) is indicated to the left.

repeat region over a wide range of concentrations *in vitro*. Binding constants were determined in physiological conditions and at concentrations likely to be found in pyramidal cells (3, 4). In contrast, previous studies of filament assembly *in vitro* have used largely unphysiological conditions and/or concentrations of tau in excess of 1 μM (14–20, 24, 25). We have shown that the core PHF–tau fragment binds full-length tau with an affinity comparable to a strong antibody–antigen interaction, and that regions of the molecule outside the core fragment do not enhance the binding constant. Self-aggregation confers proteolytic stability to a short segment, which excludes the N-terminal half of the molecule and reproduces the characteristic Glu-391 truncation at the C terminus. Truncated aggregates generated *in vitro* retain the capacity to propagate tau capture and to seed the further accumulation of truncated tau in the presence of proteases.

If high-affinity binding through the repeat domain were all that is necessary for the structural and proteolytic stability of the PHF core, a compound that blocked the tau–tau binding interaction *in vitro* might be expected to reverse these properties in PHFs isolated from the brain. We demonstrate that this is indeed the case using MB, a phenothiazine that has been used clinically (42, 43) and is known to penetrate pyramidal cells after systemic administration *in vivo* (48). As MB is inhibitory at a higher concentration than may be achieved clinically, further medicinal chemistry is required to identify more effective compounds. However, as electron microscopy and biochemical analyses of PHFs are difficult to quantify, these techniques are unsuitable as pharmaceutical screening tools.

Having demonstrated that we can model the properties of tau binding, proteolytic stability, truncation, and propagation of tau capture *in vitro*, we determined the feasibility of using the tau–tau binding assay to screen for more potent inhibitors. We show that clinically unused desmethyl derivatives of MB can be identified that are 30-fold more potent, acting at concentrations close to equimolar with respect to tau, and with K_i values in the nM range. Conversely, the side groups added

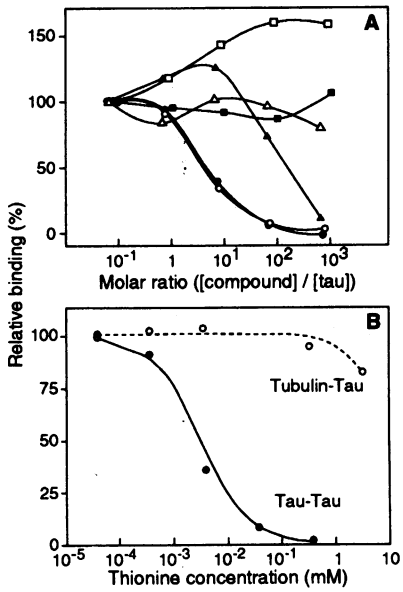

FIG. 7. (*A*) Identification of inhibitors of tau–tau binding through the repeat domain. Truncated tau protein was used at 489 nM in both aqueous (dGAE) and solid (dGA) phases of the assay, and binding was detected by mAb 423 as in Fig. 1*A*. Two of the potent phenothiazine inhibitors (thionine, ○; Azure A, ●) are shown producing linear inhibition of tau–tau binding over the range from 1:1 to 10:1 molar ratio with respect to tau. These are desmethyl derivatives of MB (▲), which is itself inhibitory only at molar ratios greater than 30:1. The neuroleptic phenothiazine chlorpromazine (△) and the anticholinesterase tacrine (■), used clinically in AD, are inactive as inhibitors of tau–tau binding through the repeat domain. The anti-epileptic carbamazepine (□) potentiated tau–tau binding. Spline curves were fitted to data points. (*B*) Selective inhibition of tau–tau binding by thionine. Tau–tau binding was inhibited with a K_i of 98 nM (●). In a tau–tubulin assay (○), in which depolymerized tubulin was coated at 200 nM and full-length tau was incubated at 400 nM, the K_i was 7.86 mM. All data points represent means of quadruplicate measurements.

to the phenothiazine nucleus to achieve neuroleptic activity (e.g., chlorpromazine) abolish inhibitory activity. Inhibitors of tau–tau binding do not affect the physiological tau–tubulin binding interaction, which also occurs through the repeat domain. This important pharmacological distinction further confirms that tau–tau binding within PHFs is mediated by domains that differ from those involved in the normal interaction between tau and tubulin (21, 22). By contrast, hyperphosphorylation of tau does not discriminate between the two binding interactions, and pharmaceutical approaches aiming to inhibit kinases may prove both counter-productive and unnecessary (4).

In this study, we demonstrate that progressive accumulation of proteolytically stable truncated tau aggregates like those found in the brain depends on a high-affinity tau–tau binding interaction through the repeat region, and that inhibition of this interaction is associated with a reversal in the proteolytic

Table 2. Inhibitory constants for compounds in Tau–Tau and Tau–tubulin binding assays

Compound	Tau–Tau binding	Tau–tubulin binding
Thionine	98 nM	7.86 mM
Azure A	108 nM	>10 mM
Tolonium chloride	69 nM	
Azure B	112 nM	
MB	3.4 μM	
Chlorpromazine	55.9 μM	
Tacrine	>100 μM	

stability of PHFs isolated from the brain. We report selective inhibition of tau aggregation by diaminophenothiazines, which have K_i values in the nanomolar range, but for which toxicological and pharmacokinetic data are unavailable. Our results indicate the potential for pharmaceutical development of compounds that could be used to facilitate the proteolytic degradation of tau aggregates and prevent the further propagation of tau capture in AD.

We express our gratitude to Prof. John Mattick who suggested the repetitive binding/digestion experiment, and to Drs. Claudia Caputo and Jim Resch for suggesting MB and Alcec Blue as alternatives to Alcian Blue. Depolymerized bovine tubulin was kindly donated by Dr. J. Kilmartin. Some of the data presented in Figs. 2 and 3 has been reproduced (13). This work was supported by the Medical Research Council (United Kingdom), the Wellcome Trust, the Leopold Müller Estate, and the Newton Trust (Trinity College).

1. Wischik, C. M., Novak, M., Thogersen, H. C., Edwards, P. C., Runswick, M. J., Jakes, R., Walker, J. E., Milstein, C., Roth, M. & Klug, A. (1988) *Proc. Natl. Acad. Sci. USA* **85,** 4506–4510.
2. Harrington, C. R., Mukaetova-Ladinska, E. B., Hills, R., Edwards, P. C., Montejo de Garcini, E., Novak, M. & Wischik, C. M. (1991) *Proc. Natl. Acad. Sci. USA* **88,** 5842–5846.
3. Mukaetova-Ladinska, E. B., Harrington, C. R., Roth, M. & Wischik, C. M. (1993) *Am. J. Pathol.* **143,** 565–578.
4. Lai, R. Y. K., Gertz, H.-J., Wischik, D. J., Xuereb, J. H., Mukaetova-Ladinska, E. B., Harrington, C. R., Edwards, P. C., Mena, R., Paykel, E. S., Brayne, C., Huppert, F. A., Roth, M. & Wischik C. M. (1995) *Neurobiol. Aging* **16,** 433–445.
5. Bondareff, W., Wischik, C. M., Novak, M., Amos, W. B., Klug, A. & Roth, M. (1989) *Am. J. Pathol.* **137,** 711–723.
6. Kosik, K. S., Orecchio, L. D., Binder, L., Trojanowski, J. Q., Lee, V. M.-Y. & Lee, G. (1988) *Neuron* **1,** 817–825.
7. Mena, R., Edwards, P. C., Harrington, C. R., Mukaetova-Ladinska, E. B. & Wischik, C. M. (1996) *Acta Neuropathol.* **91,** 633–641.
8. Mena, R., Wischik, C. M., Novak, M., Milstein, C. & Cuello, A. C. (1991) *J. Neuropathol. Exp. Neurol.* **50,** 474–490.
9. Bondareff, W., Mountjoy, C. Q., Wischik, C. M., Hauser, D. L., LaBree, L. D. & Roth, M. (1993) *Arch. Gen. Psychiatry* **50,** 350–356.
10. McKee, A. C., Kowall, N. W. & Kosik, K. S. (1989) *Ann. Neurol.* **26,** 652–659.
11. Wilcock, G. K. & Esiri, M. M. (1982) *J. Neurol. Sci.* **56,** 407–417.
12. Arriagada, P. V., Marzloff, K. & Hyman, B. T. (1992) *Neurology* **42,** 1681–1688.
13. Wischik, C. M., Edwards, P. C. & Harrington, C. R. (1995) in *Neurobiology of Alzheimer's Disease*, eds. Dawbarn, D. & Allen, S. J. (Bios Scientific, Oxford), pp. 89–148.
14. Montejo de Garcini, E., Serrano, L. & Avila, J. (1986) *Biochem. Biophys. Res. Commun.* **141,** 790–796.
15. Wille, H., Drewes, G., Biernat, J., Mandelkow, E.-M. & Mandelkow, E. (1992) *J. Cell Biol.* **118,** 573–584.
16. Crowther, R. A., Olesen, O. F., Jakes, R. & Goedert, M. (1992) *FEBS Lett.* **309,** 199–202.
17. Ruben, G. C., Iqbal, K., Grundke-Iqbal, I. & Johnson, J. E., Jr. (1993) *Brain Res.* **602,** 1–13.
18. Troncoso, J. C., Costello, A., Watson, A. L., Jr., & Johnson, G. V. W. (1993) *Brain Res.* **613,** 313–316.
19. Garcia de Ancos, J., Correas, I. & Avila, J. (1993) *J. Biol. Chem.* **268,** 7976–7982.
20. Crowther, R. A., Olesen, O. F., Smith, M. J., Jakes, R. & Goedert, M. (1994) *FEBS Lett.* **337,** 135–138.
21. Jakes, R., Novak, M., Davison, M. & Wischik, C. M. (1991) *EMBO J.* **10,** 2725–2729.
22. Novak, M., Kabat, J. & Wischik, C. M. (1993) *EMBO J.* **12,** 365–370.
23. Ksiezak-Reding, H. & Yen, S.-H. (1991) *Neuron* **6,** 717–728.
24. Schweers, O., Mandelkow, E.-M., Biernat, J. & Mandelkow, E. (1995) *Proc. Natl. Acad. Sci. USA* **92,** 8463–8467.
25. Wilson, D. M. & Binder, L. I. (1995) *J. Biol. Chem.* **270,** 24306–24314.
26. Wischik, C. M., Crowther, R. A., Stewart M. & Roth, M. (1985) *J. Cell Biol.* **100,** 1905–1912.
27. Crowther, R. A. & Wischik, C. M. (1985) *EMBO J.* **4,** 3661–3665.
28. Wischik, C. M., Novak, M., Edwards, P. C., Klug, A., Tichelaar, W. & Crowther, R. A. (1988) *Proc. Natl. Acad. Sci. USA* **85,** 4884–4888.
29. Novak, M., Jakes, R., Edwards, P. C., Milstein, C. & Wischik, C. M. (1991) *Proc. Natl. Acad. Sci. USA* **88,** 5837–5841.
30. Caputo, C. B., Wischik, C. M., Novak, M., Scott, C. W., Brunner, W. F., Montejo de Garcini, E., Lo, M. M. S., Norris, T. & Salama, A. I. (1992) *Neurobiol. Aging* **13,** 267–274.
31. Goedert, M., Wischik, C. M., Crowther, R. A., Walker, J. E. & Klug, A. (1988) *Proc. Natl. Acad. Sci. USA* **85,** 4051–4055.
32. Harrington, C. R., Wischik, C. M., McArthur, F. K., Taylor, G. A., Edwardson, J. A. & Candy, J. M. (1994) *Lancet* **343,** 993–997.
33. Harrington, C. R., Louwagie, J., Rossau, R., Vanmechelen, E., Perry, R. H., Perry, E. K., Xuereb, J. H., Roth, M. & Wischik, C. M. (1994) *Am. J. Pathol.* **145,** 1472–1484.
34. Goedert, M., Spillantini, M. G., Jakes, R., Rutherford, D. & Crowther, R. A. (1989) *Neuron* **3,** 519–526.
35. Biernat, J., Gustke, N., Drewes, G., Mandelkow, E.-M. & Mandelkow, E. (1993) *Neuron* **11,** 153–163.
36. Lai, R. Y. K. (1995) Ph.D. thesis (Univ. of Cambridge, Cambridge, U.K.).
37. Harrington, C. R. (1990) *Anal. Biochem.* **186,** 285–287.
38. Harrington, C. R., Edwards, P. C. & Wischik, C. M. (1990) *J. Immunol. Methods* **134,** 261–271.
39. Goedert, M., Jakes, R., Spillantini, M.-G. & Crowther, R. A. (1994) in *Microtubules*, eds. Hyams, J. S. & Lloyd, C. W. (Wiley/Liss, New York), pp. 183–200.
40. Trojanowski, J. Q. & Lee, V. M.-Y. (1995) *FASEB J.* **9,** 1570–1576.
41. Resch, J. F., Lehr, G. S. & Wischik, C. M. (1991) *Bioorg. Med. Chem. Lett.* **10,** 519–522.
42. Di Santo, A. R. & Wagner, J. G. (1972) *J. Pharm. Sci.* **61,** 1086–1094.
43. Naylor, G., Martin, S. E., Hopwood, S. E. & Watson, Y. (1986) *Biol. Psychiatry* **21,** 915–920.
44. Sherrington, R., Rogaev, E. I., Liang, Y., Rogaeva, E. A., Levesque, G., *et al.* (1995) *Nature (London)* **373,** 754–760.
45. Levy-Lahad, E., Wasco, W., Poorkaj, P., Romaro, D. M., Oshima, J., *et al.* (1995) *Science* **269,** 973–977.
46. Mukaetova-Ladinska, C. R., Harrington, M., Roth, C. M. & Wischik, C. M. (1994) *Dev. Brain Dysfunct.* **7,** 311–329.
47. Jobst, K. A., Smith, A. D., Szatmari, M., Esiri, M. M., Jaskowski, A., Hindley, N., McDonald, B. & Molyneux, A. J. (1994) *Lancet* **343,** 829–830.
48. Muller, T. (1992) *Acta Anat.* **144,** 39–44.